DOI: 10.1002/ejic.200800911

Hydrothermal Synthesis of Three-Dimensional Hierarchical CuO Butterfly-Like Architectures

Yajing Zhang,[a,b] Siu Wing Or,*[b] Xiaolei Wang,[a] Tieyu Cui,[a] Weibin Cui,[a] Ying Zhang,[a] and Zhidong Zhang[a]

Keywords: Hydrothermal synthesis / Copper oxide / Nanostructures / Self-assembly

Uniform 3D hierarchical CuO butterfly-like architectures were fabricated by a surfactant-assisted hydrothermal oriented attachment route. This route included the formation of CuO butterfly-like architectures in a solution of cupric chloride ($CuCl_2 \cdot 2H_2O$) and sodium hydroxide (NaOH) at 100 °C for 15 h by using sodium dodecyl benzenesulfonate (SDBS) as surfactant. The as-prepared CuO architecture was characterized by X-ray diffraction, scanning electron microscopy and transmission electron microscopy. The CuO butterfly-like architectures, with lengths of about 6 μm and widths of 2–4 μm, were assembled from several tens of oriented attachment rhombic nanosheets with a thickness of about 60 nm. A growth mechanism for the formation of the CuO butterfly-like architectures was proposed on the basis of time-dependent experiments. The synthetic parameters such as reaction temperature, the concentration of sodium hydroxide and reaction time all affected the morphology of the CuO architectures. The synthetic strategy could be extended to assemble 3D architectures of other materials.

Introduction

Synthesis of hierarchical micro- and/or nanomaterials, self-assembled by ordered alignment of nanobuilding blocks, has attracted much attention due to their novel properties and potential application in optics, electronics, magnetics and biology.[1] As a result, a number of micro- and/or nanomaterials with hierarchical structures, including metals, metal oxide, hydrate, sulfide, copolymers and other materials,[2–6] have been fabricated by different driving mechanisms, including surface tension, electric and magnetic forces, and hydrophobic interactions.[7–9] However, synthesis of novel hierarchical structured micro- and/or nanomaterials is still an interesting topic, because they can exhibit new physicochemical behaviours and provide much promise for the fabrication of materials with advanced functionalities.

Cupric oxide, as an important *p*-type semiconductor with a narrow bandgap (E_g = 1.2 eV), has been extensively investigated for its application in solar energy conversion, lithium-ion batteries, gas sensors, field emission and catalysis.[10–13] Because there is a close relationship between the bandgap energies of CuO nanostructures and their shapes and sizes, different synthetic routes including vapour–solid, vapour–liquid–solid and solid–liquid routes were developed for the synthesis of CuO.[14] Various CuO micro- and/or nanomaterials, such as nanoparticles,[15] one-dimensional (1D) nanotubes, nanorods, nanobelts and nanoneedles,[16,17] two-dimensional (2D) nanoribbions, nanosheets, nanoleaves and nanowiskers,[18] three-dimensional (3D) microflowers and microbranches formed through the self-assembly of nanometre-sized building blocks,[19] have been synthesized by these routes. For example, CuO nanowires supported on various substrates were obtained by the thermal oxidation of these substrates in air.[20] CuO nanotubes and nanorods were synthesized by controlling the concentration of the precursor.[21] The formation of CuO rod-like, flake-like and branch-like nanostructures was achieved by adjusting the molar radio of sodium citrate to cupric salts.[22] CuO nanoribbons and nanorings were synthesized by a surfactant-assisted hydrothermal route for different reaction times.[23] CuO nanoleaves were fabricated by hierarchical oriented attachment of $Cu(OH)_2$ nanowires.[24] For 3D hierarchical CuO micromaterials with two or more levels of structure, their nanometre-sized building blocks provide a high surface area, whereas their whole micrometre-sized structure provides sufficient mechanical properties, so the combination of these features will improve their electrochemical performance and adsorption ability (removal of heavy metal ions)[25,26] However, 3D hierarchical CuO micromaterials have seldom been reported. Zeng et al. assembled hollow dandelion-like CuO microspheres com-

[a] Shenyang National Laboratory for Materials Science, Institute of Metal Research and International Centre for Materials Physics, Chinese Academy of Sciences,
Shenyang 110016, P. R. China
[b] Department of Electrical Engineering, The Hong Kong Polytechnic University,
Hung Hom, Kowloon, Hong Kong
E-mail: eeswor@polyu.edu.hk

Supporting information for this article is available on the WWW under http://www.eurjic.org or from the author.

posed of rhombic nanobuilding blocks through the oriented aggregation of smaller nanoribbons by a two-step procedure with the use of ethanol as solvent.[27] Xu et al. fabricated CuO microflowers composed of nanosheets in ammonia solution.[28] Nevertheless, to the best of our knowledge, 3D hierarchical CuO butterfly-like architectures have not been reported.

Here we report the controlled synthesis of 3D hierarchical butterfly-like CuO architectures by a surfactant-assisted hydrothermal oriented attachment route. The effects of the reaction parameters, such as the reaction temperature, reaction time and the concentration of NaOH, on the morphologies of CuO are investigated. The growth mechanism of the 3D hierarchical CuO butterfly-like architectures is proposed on the basis of the results of systematic time-dependent experiments. The CuO butterfly-like architectures provide a supplement of available 3D CuO architectures, and it can be expected to extend for assembling new electronic and optoelectronic micro- and/or nanodevices.

Results and Discussion

Synthesis and Characterization of Hierarchical CuO Butterfly-Like Architectures

The X-ray diffraction (XRD) patterns of the precursor, the intermediate and the final products are shown in Figure 1. Figure 1a is the XRD pattern of the precursor, in which all the peaks can be indexed to orthorhombic $Cu(OH)_2$ (JCPDS No. 13-0420). Figure 1d shows the XRD pattern of the final product obtained at 100 °C after 15 h hydrothermal treatment, in which all the XRD peaks can be indexed to monoclinic CuO, which is consistent with the standard card JCPDS No.48–1548 (space group *C*2/*c*; a = 4.688 Å, b = 3.423 Å, c = 5.132 Å). Impurities were obviously not found in the final product, indicating it is pure CuO. Figure 1b [the mixture of $Cu(OH)_2$ and CuO] and Figure 1c (CuO) are the XRD patterns of the products as-prepared at 100 °C after 1 and 5 h, respectively. The XRD results confirm that the final product of CuO is transformed from the initial precursor of $Cu(OH)_2$. The energy-dispersive spectrum (EDS) result reveals that only the Cu and O elements are contained in the final product, and the atomic ratio of Cu to O in the product is about 1:1 (49:51), as shown in Figure 2. The EDS result further confirms that the final product is only CuO (Au element originates from the thin Au layer sputtering on the sample in the test).

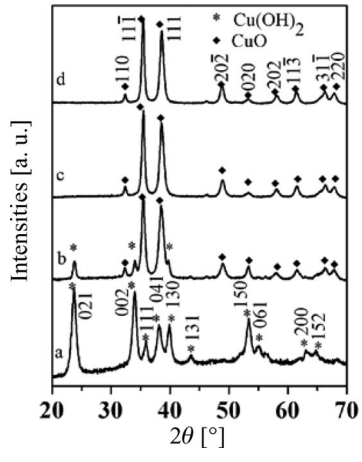

Figure 1. XRD patterns of (a) the precursor of $Cu(OH)_2$ and the products collected at 100 °C for (b) 1 h, (c) 5 h and (d) 15 h.

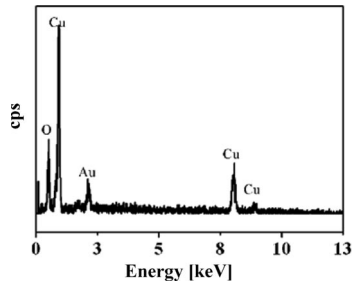

Figure 2. EDS pattern of the as-prepared CuO butterfly-like architectures at 100 °C for 15 h.

Figure 3 shows the typical morphology of the final CuO product with different magnifications. The low-magnification scanning electron microscopy (SEM) (Figure 3a) image implies that the final CuO product is highly uniform butterfly-like architectures, with a length of about 6 μm and width of 2–4 μm. The magnified SEM image (Figure 3b) shows that the CuO butterfly-like architectures are composed of several tens of order-attached rhombic nanosheets, which can be classified as a hierarchical structure. The nanosheets are about 60 nm thick, as estimated from the side view of the architecture (Figure 3c). It is also observed that the CuO nanosheets attach together in the middle part of an

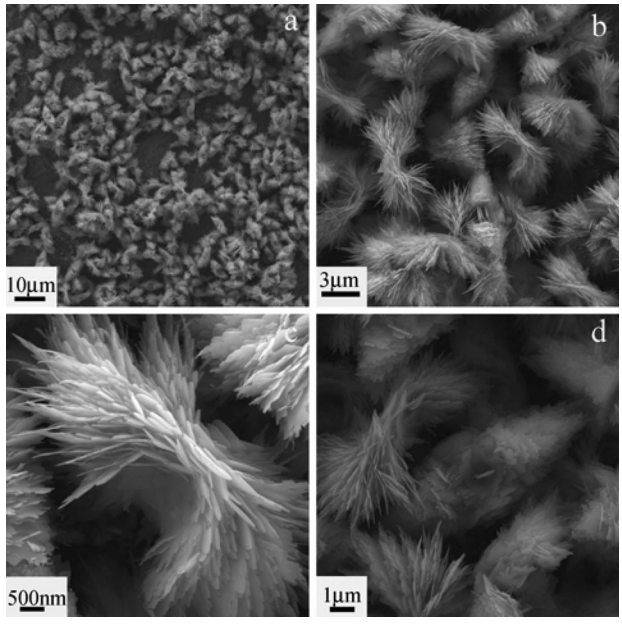

Figure 3. (a) Low-magnification and (b) high-magnification SEM images of the CuO butterfly-like architectures prepared at 100 °C for 15 h; (c) side view and (d) top view of an individual CuO butterfly-like architecture.

individual butterfly-like architecture, and they become curly and separate at the two ends. Furthermore, the two ends exhibit a symmetrical character, as displayed in the top-view image (Figure 3d). The BET surface area for the CuO butterfly-like architectures is about 17 $m^2 g^{-1}$, which is smaller than that of the hollow dandelion-like CuO.[27] This is attributed to the fact that the middle part of the butterfly-like architectures attach densely together. It is worth mentioning that the hierarchical CuO butterfly-like architectures are very stable and still maintain the morphology after ultrasonication for 30 min.

Growth Mechanism for the Formation of the CuO Butterfly-Like Architectures

To understand the growth mechanism of the CuO butterfly-like architectures, systematic time-dependent experiments were carried out at 100 °C. The SEM and TEM images (Figure 4) of the products obtained after 1, 5 and 10 h in the hydrothermal process illustrate the evolution of the morphology of the butterfly-like CuO architectures. When the reaction time is 1 h, 1D nanoribbons, with widths of 50–60 nm and lengths of 1–2 μm, are observed as the dominant product, although several 2D rhombic nanosheets are also detected (shown by white arrow in Figure 4a). An individual nanosheet is about 500 nm in width and 1–2 μm in length. It can be obviously observed that the nanosheet is assembled by the ordered attachment of several nanoribbons. TEM results (Figure 4b) further confirm the morphologies of the nanoribbons and rhombic nanosheets, and those monodispersive nanoribbons are very flexible and tend to curve. The corresponding select area electron diffraction (SAED) of the nanosheet (the top square part shown in Figure 4b) is shown in Figure 4c. The diffraction pattern can be indexed to (020), (11$\bar{1}$) and (20$\bar{2}$) planes of CuO, and the obvious symmetry arc-like diffraction spots illustrate that the nanosheet is assembled by oriented building blocks.[3b] Figure 4d is the SAED result of an individual nanoribbon (the bottom square part shown in Figure 4b), revealing the single-crystal nature of the nanoribbon, and the SAED spots can also be determined to be (020), (11$\bar{1}$) and (20$\bar{2}$) planes of CuO. The results further indicate that the nanosheets are formed by oriented attachment of CuO nanoribbons. This is in agreement with the earlier reports.[23,24,27] No nanoribbons are found in the product obtained after 5 h (Figure 4e), but 2D rhombic nanosheets (shown by arrows) and 3D undeveloped butterfly-like architectures are observed. When the reaction is prolonged for 10 h, more 3D perfect butterfly-like architectures are yielded, whereas the number of 2D nanosheets becomes less, as shown in Figure 4f. It is found that 15 h is sufficient for generating well-developed CuO butterfly-like architectures, and nearly no individual 2D nanoleaves can be observed (Figure 2).

On the basis of above experimental results and the literature,[21,23,24] a growth mechanism for the formation of the CuO butterfly-like architectures is proposed, as schemed in Figure 5. The formation of the architectures possibly consists of four main steps: (1) Formation of $Cu(OH)_2$ crystal nuclei (step a). (2) CuO nuclei form by the decomposition of $Cu(OH)_2$ and grow into CuO nanoribbons (step b). (3) The CuO nanoribbons self-assemble into CuO rhombic nanosheets through an oriented attachment mechanism (step c). (4) CuO nanosheets attach orderly and assemble into hierarchical butterfly-like architectures (step d). The oriented attachment in both steps c and d are driven by eliminating higher surface energies.

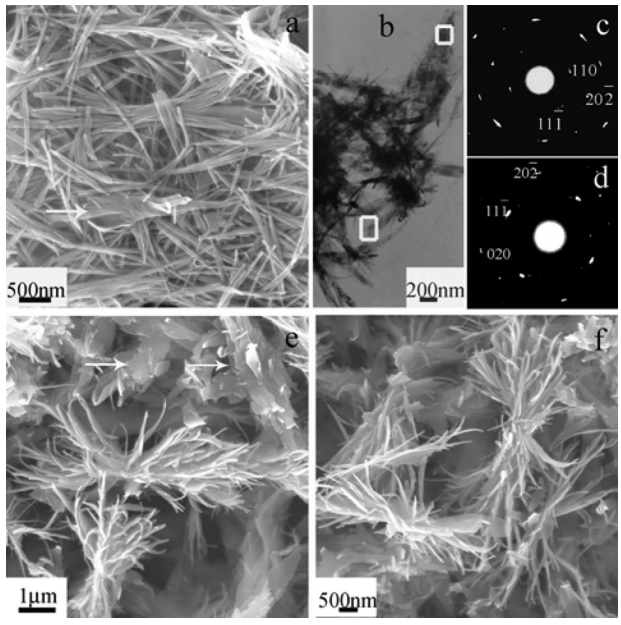

Figure 4. (a) SEM and (b) TEM images of the products prepared at 100 °C for 1 h; (c) the corresponding SAED pattern of the top part of the rhombic nanosheet (shown by top square in Figure 4b); (d) the corresponding SAED pattern of the top part of the nanowire (shown by bottom square in Figure 4b); (e) SEM images of the products prepared at 100 °C for 5 h and (f) 10 h.

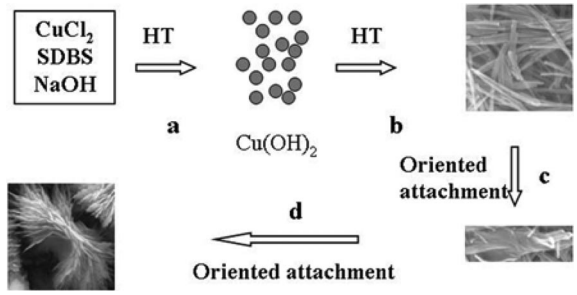

Figure 5. Schematic illustration of the formation procedure of the 3D CuO butterfly-like architectures.

To determine the role of SDBS in the formation process of CuO butterfly-like architectures, time-dependent experiments were also carried out at 100 °C in the absence of SDBS, while keeping other reaction parameters unchanged. The results show that: (1) CuO nanoribbons did not form during the reaction process (Figure S1, Supporting Information). (2) The final CuO product consisted of a majority of 3D shuttle-like architectures and a minority of 2D flat

nanosheets. The results indicate that the SDBS surfactant plays a critical role in the formation of CuO nanoribbons. The nanoribbons tend to curve, because they are flexible and thin, and hence, they are prerequisite building blocks for assembling intermediate curved CuO nanosheets and then final butterfly-like architectures. The group of Qian proposed a crystal-splitting mechanism for forming CuO nanoribbons, wherein SDBS directly interacts with the surfaces of CuO flakes and subsequently its intense Brownian movement leading to CuO flakes split into CuO nanoribbons.[23] It is understood on the basis of our experimental results that SDBS in our reaction system plays the same role. In the presence of SDBS, the Cu^{2+} cations could directly attach to the DBS^- anions and produce $Cu(DBS)_2$, then $Cu(DBS)_2$ reacts with NaOH to form CuO. The whole reaction process can be described by Equations (1) and (2).[23]

$$Cu(DBS)_2 + 4OH^- \rightarrow [Cu(OH)_4]^{2-} + 2DBS^- \quad (1)$$

$$[Cu(OH)_4]^{2-} \rightarrow CuO + H_2O + 2\ OH^- \quad (2)$$

SDBS was also substituted with other surfactants such as sodium dodecyl sulfate (SDS), cetyltrimethylammonium bromide (CTAB) and poly(vinylpyrrolidone) (PVP). When SDS was used as surfactant, the butterfly-like architectures were also obtained (Figure 6a). In the case of CTAB and PVP, the products were poorly defined butterfly-like architectures with densely attached nanosheets and flat nanosheets, as shown in Figure 6b and c, respectively. The results demonstrate that the anionic surfactants are more favourable for achieving well-defined butterfly-like architectures in comparison to cationic and neutral surfactants. This may be ascribed to the direct interaction of anionic surfactants, such as SDBS and SDS, with cupric ions or to anion-selective adsorption on the CuO surface in solution. Cationic and nonionic surfactants, such as CTAB and PVP, cannot produce butterfly-like architectures possibly because of their weak interaction with cupric ions.[29]

In addition, the effect of the concentration of NaOH on the morphology of the final CuO product was examined. In the controlled experiments, when the concentration of NaOH was 2 M, it did not form any butterfly-like structures; rather, shuttle-like architectures were formed by compact attached nanosheets (Figure 7a). A further increase in the concentration of NaOH to 5 M, resulted in the formation of spherical architectures composed of a number of nanosheets (Figure 7b). It can be concluded that a low concentration of NaOH is critical for the formation of CuO butterfly-like architectures. This can also be explained by the formation model proposed in Figure 5. When the concentration of NaOH in the solution is increased, the reaction rate is accelerated according to Equations (1) and (2), which leads to the formation of much thicker and less flexible nanoribbons in a short time; subsequently, they self-assemble in an oriented manner into flat and thick nanosheets instead of curved nanosheets. Finally, the flat nanosheets self-assemble in an oriented manner into CuO shuttle-like architectures. The concentration of NaOH is high enough (e.g., 5 M) in solution, and hence, the reaction rate is excessively fast, but the flat nanosheets cannot perform oriented self-assembly at such a fast reaction rate, so instead they attach randomly and form CuO flower-like architectures.

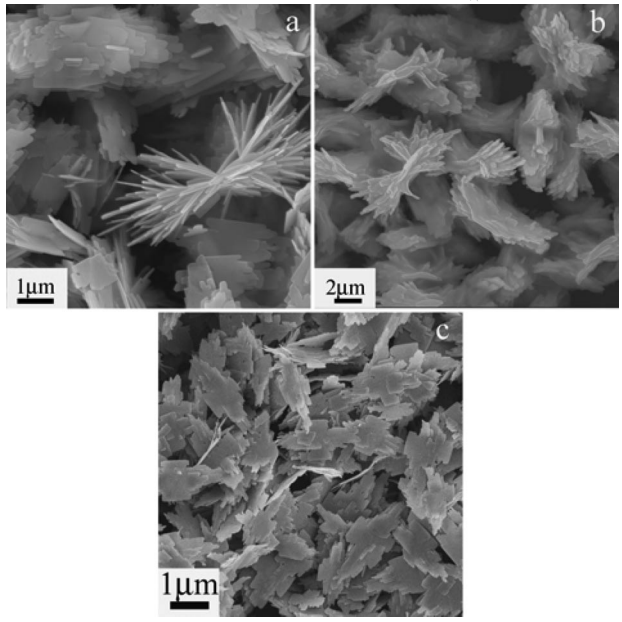

Figure 6. SEM images of the products prepared in the presence of (a) SDS, (b) CTAB and (c) PVP.

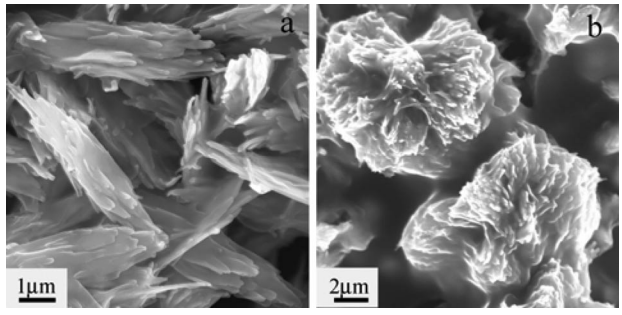

Figure 7. SEM images of the products prepared at 100 °C with different concentrations of NaOH: (a) 2 M and (b) 5 M.

Apart from the concentration of NaOH, the reaction temperature affects the morphology of the final CuO product. The controlled experiments demonstrated that a high reaction temperature is not favourable for the self-assembly of CuO butterfly-like architectures, but favours the formation of other 3D architectures. For instance, when the reaction is carried out at 120 and 140 °C, irregular structures form by random aggregation of nanoribbons, instead of oriented attachment of nanosheets (Figure 8a and b). A further increase in the reaction temperature (160 and 180 °C) leads to the formation of isotropic flower-like architectures, which are created through the self-assembly of many nanoribbons (Figure 8c and d). At a relatively low temperature, such as 80 °C (Figure S2, Supporting Information), CuO butterfly-like architectures can also be obtained, but need a relatively long reaction time. According to our proposed

formation model in Figure 5, it is understandable that isotropic spherical (or near-spherical) architectures are achieved at higher reaction temperatures, because the reaction rate rises with increasing temperature, and accordingly, more intermediate building blocks of nanoribbons are produced in a shorter reaction time, and together with the intense Brownian movement, this results in random aggregation instead of oriented attachment.[30] This is consistent with previous reports.[2f,27] The results reveal that the morphology of the product is strongly determined by the reaction temperature.

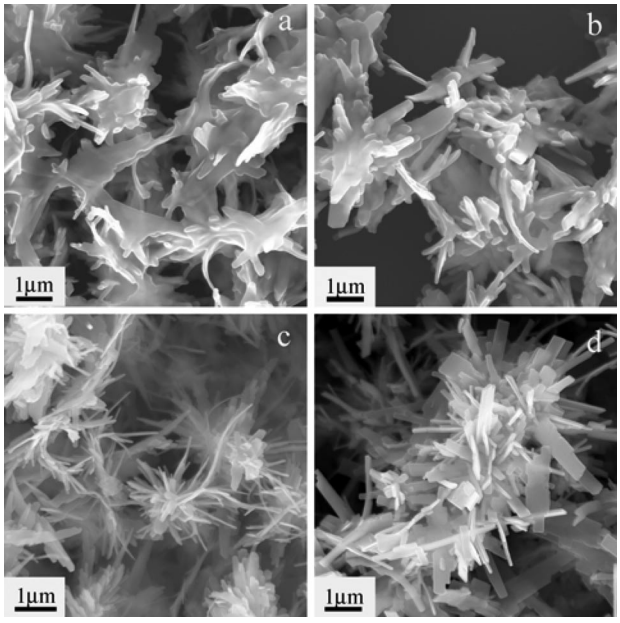

Figure 8. SEM images of the products prepared at different reaction temperatures: (a) 120 °C, (b) 140 °C, (c) 160 °C and (d) 180 °C for 15 h.

Conclusions

3D hierarchical CuO butterfly-like architectures composed of several tens of rhombic nanosheets were fabricated by a hydrothermal oriented attachment route. Experimental results suggest that the reaction temperature, the concentration of NaOH and the reaction time all influence the morphology of CuO, and the SDBS surfactant plays a key role in the formation of the CuO architectures. In addition, the CuO butterfly-like architectures were found to self-assemble through an oriented attachment mechanism. Our synthetic approach can be employed to fabricate 3D hierarchical architectures of other materials under appropriate conditions.

Experimental Section

General: All reagents were commercially available in analytical purity and used without further purification. In a typical procedure, $CuCl_2 \cdot 2H_2O$ (0.34 g, 2 mmol), SDBS (0.232 g, 1 mmol) and NaOH (1.6 g, 40 mmol) were first dissolved in distilled water (40 mL) under constant stirring, and the precursor blue suspension was obtained. For obtaining the precursor, the initial blue suspension was placed static for several hours in air and then the blue precipitate was separated, washed and dried for characterization. For preparing the 3D hierarchical butterfly-like CuO architectures, the initial blue suspension was transferred into a 50-mL Teflon-lined stainless steel autoclave. The autoclave was sealed and heated at 100 °C for 15 h and then cooled to room temperature naturally. The products obtained after hydrothermal treatment were centrifuged, washed with distilled water and ethanol several times and finally dried in vacuo at 60 °C for 4 h. Control experiments were carried out by adjusting the reaction temperature (80–180 °C) and the amount of NaOH (1–5 M), while other reaction parameters were left unchanged.

The phases of all the products were identified with a Rigaku D/max 2500 pc X-ray diffractometer (XRD) with Cu-K_α radiation (λ = 1.54156 Å) at a scan rate of 0.04°s^{-1}. The morphology was investigated with a Supra 35 field-emission scanning electron microscope (FESEM) equipped with energy-dispersive spectrum (EDS) operated at an acceleration voltage of 20 kV. The Brunauer-Emmett-Teller (BET) surface area was measured by the nitrogen adsorption–desorption method by using a Micromeritics (ASAP2010M) analyzer. Transmission electron microscopy (TEM) observation was carried out with a TECNAI 20 with an emission voltage of 200 kV. For sample preparation for FESEM and TEM observations, at first, a small amount of the as-prepared products was dispersed in ethanol by ultrasonic treatment for 10 min, and then one drop of the colloidal solution was deposited onto Si wafer and Cu grids coated with a carbon layer, respectively.

Supporting Information (see footnote on the first page of this article): SEM images of the products prepared at 100 °C without SDBS for different reaction time; SEM image of the products prepared at 80 °C for different reaction time.

Acknowledgments

This work was supported by the National Nature Science Foundation of China (Projects No. 50331030 and No.50703046), the Research Grants Council of the HKSAR Government (PolyU 5257/06E) and the Central Research Grant of The Hong Kong Polytechnic University (A-PA3C).

[1] a) H. G. Yang, H. C. Zeng, *Angew. Chem. Int. Ed.* **2004**, *43*, 5930–5933; b) A. D. Dinsmore, M. F. Hsu, M. G. Nikolaides, M. Marquez, A. R. Bausch, D. A. Weitz, *Science* **2002**, *298*, 1006–1009.

[2] a) Y. C. Zhu, Q. Yang, H. G. Zheng, W. C. Yu, Y. T. Qian, *Mater. Chem. Phys.* **2005**, *91*, 293–297; b) Y. L. Hou, H. Kondoh, T. Ohta, *Chem. Mater.* **2005**, *17*, 3994–3996; c) L. Guo, F. Liang, X. G. Wen, S. H. Yang, L. He, W. Z. Zheng, C. P. Chen, Q. P. Zhong, *Adv. Funct. Mater.* **2007**, *17*, 425–430; d) L. P. Zhu, H. M. Xiao, W. D. Zhang, Y. Yang, S. Y. Fu, *Cryst. Growth Des.* **2008**, *8*, 1113–1118; e) Y. J. Zhang, S. Ma, D. Li, Z. H. Wang, Z. D. Zhang, *Mater. Res. Bull.* **2008**, *43*, 1957–1965; f) Y. J. Zhang, Y. Zhang, Z. H. Wang, D. Li, T. Y. Cui, W. Liu, Z. D. Zhang, *Eur. J. Inorg. Chem.* **2008**, *17*, 2733–2738.

[3] a) Z. Fang, K. B. Tang, J. M. Shen, G. Z. Shen, Q. Yang, *Cryst. Growth Des.* **2007**, *7*, 2254–2257; b) Y. Y. Li, J. P. Liu, X. T. Huang, G. Y. Li, *Cryst. Growth Des.* **2007**, *7*, 1350–1355; c) Z. Y. Yuan, A. Vantomme, A. Leonard, B. L. Su, *Chem. Commun.* **2003**, 1558–1559; d) J. Y. Lao, J. Y. Huang, D. Z. Wang, Z. F. Ren, *J. Mat. Chem.* **2004**, *14*, 770–773; e) R. S. Yuan, X. Z. Fu, X. C. Wang, P. Liu, L. Wu, Y. M. Xu, X. X. Wang, Z. Y. Wang, *Chem. Mater.* **2006**, *18*, 4700–4705; f) D. Yan, P. X.

Yan, G. H. Yue, J. Z. Liu, J. B. Chang, Q. Yang, D. M. Qu, Z. R. Geng, J. T. Chen, G. A. Zhang, R. F. Zhuo, *Chem. Phys. Lett.* **2007**, *440*, 134–138.
[4] a) L. X. Yang, Y. J. Zhu, L. Li, L. Zhang, H. Tong, W. W. Wang, G. F. Cheng, J. F. Zhu, *Eur. J. Inorg. Chem.* **2006**, 4787–4792; b) D. B. Wang, C. X. Song, Z. S. Hu, X. Fu, *J. Phys. Chem. B* **2005**, *109*, 1125–1129; c) J. P. Huang, X. T. Huang, Y. Y. Li, K. M. Sulieman, X. He, F. L. Sun, *J. Phys. Chem. B* **2006**, *110*, 21865–21872.
[5] a) G. Z. Shen, Y. Bando, J. Q. Hu, D. Golberg, *Appl. Phys. Lett.* **2007**, *90*,123101; b) X. L. Li, J. P. Ge, Y. D. Li, *Chem. Eur. J.* **2004**, *10*, 6163–6167; c) Y. R. Ma, L. M. Qi, J. M. Ma, H. M. Chen, *Cryst. Growth Des.* **2004**, *4*, 351–354; d) D. Moore, Y. Ding, Z. L. Wang, *Angew. Chem. Int. Ed.* **2006**, *45*, 5150–5154; e) Y. Cheng, Y. S. Wang, C. Jia, F. Bao, *J. Phys. Chem. B* **2006**, *110*, 24399–24402; f) Q. Z. Yao, G. Jin, G. T. Zhou, *Mater. Chem. Phys.* **2008**, *109*, 164–168.
[6] a) H. Kang, F. A. Detcheverry, A. N. Mangham, M. P. Stoykovich, K. C. Daoulas, R. J. Hamers, M. Muller, J. J. D. Pablo, P. F. Nealey, *Phys. Rev. Lett.* **2008**, *100*, 148303; b) W. A. Lopes, H. M. Jaeger, *Nature* **2001**, *414*, 735–738; c) D. Sundrani, S. B. Darling, S. J. Sibener, *Langmuir* **2004**, *20*, 5091–5099.
[7] a) X. W. Teng, H. Yang, *Nano Lett.* **2005**, *5*, 885–891; b) X. S. Fang, C. H. Ye, L. D. Zhang, J. X. Zhang, J. W. Zhao, P. Yan, *Small* **2005**, *1*, 422–428.
[8] a) L. Manna, D. J. Milliron, A. Meisel, E. C. Scher, A. P. Alivisatos, *Nat. Mater.* **2003**, *2*, 382–385; b) H. Q. Yan, R. R. He, J. Johnson, M. Law, R. J. Saykally, P. D. Yang, *J. Am. Chem. Soc.* **2003**, *125*, 4728–4729; c) F. Gao, Q. Y. Lu, S. H. Xie, D. Y. Zhao, *Adv. Mater.* **2002**, *14*, 1537–1540.
[9] a) C. B. Murray, C. R. Kagan, M. G. Bawendi, *Science* **1995**, *270*, 1335–1338; b) J. Liu, Q. Wu, Y. Ding, *Cryst. Growth Des.* **2005**, *5*, 445–449.
[10] a) S. Anandan, X. G. Wen, S. H. Yang, *Mater. Chem. Phys.* **2005**, *93*, 35–40; b) M. Serra, D. Sainz, *Sol Energy Mater.* **1986**, *13*, 463–468.
[11] a) X. P. Gao, J. L. Bao, G. L. Pan, H. Y. Zhu, P. X. Huang, F. Wu, D. Y. Song, *J. Phys. Chem. B* **2004**, *108*, 5547–5551; b) A. Debart, L. Dupont, P. Poizot, J. B. Leriche, J. M. Tarascon, *J. Electrochem. Soc.* **2001**, *148*, A1266–A1274; c) S. Q. Wang, J. Y. Zhang, C. H. Chen, *Scrip. Mater.* **2007**, *57*, 337–340; d) D. W. Zhang, T. H. Yi, C. H. Chen, *Nanotechnology* **2005**, *16*, 2338–2341.
[12] a) J. T. Zhang, J. F. Liu, Q. Peng, X. Wang, Y. D. Li, *Chem. Mater.* **2006**, *18*, 867–871; b) C. T. Hsieh, J. M. Chen, H. H. Lin, H. C. Shih, *Appl. Phys. Lett.* **2003**, *83*, 3383–3387; c) Y. W. Zhu, T. Yu, F. C. Cheong, X. J. Xui, C. T. Lim, V. B. C. Tan, J. T. L. Thong, C. H. Sow, *Nanotechnology* **2005**, *16*, 88–92; d) R. B. Vasiliev, M. N. Rumyantseva, N. V. Yakovlev, A. M. Gaskov, *Sens. Actutors B* **1998**, *50*, 186–193; e) X. H. Kong, Y. D. Li, *Sens. Actutors B* **2005**, *105*, 449–453; f) V. R. Katti, A. K. Debnath, K. P. Muthe, M. Kaur, A. K. Dua, S. C. Gadkari, S. K. Gupta, V. C. Sahni, *Sens. Actutors B* **2003**, *96*, 245–252.
[13] a) K. B. Zhou, R. P. Wang, B. Q. Xu, Y. D. Li, *Nanotechnology* **2006**, *17*, 3939–3943; b) A. Santos, P. Yustos, A. Quintanilla, G. Ruiz, F. Garcia-Ochoa, *Appl. Catal. B: Environ.* **2005**, *61*, 323–333; c) H. G. El-Shobaky, M. Mokhtar, G. A. El-Shobaky, *Appl. Catal. A: Gen.* **1999**, *61*, 335–344; d) W. H. Shen, X. P. Dong, Y. F. Zhu, H. R. Chen, J. L. Shi, *Microporous Mesoporous Mater.* **2005**, *85*, 157–162.
[14] S. Anandan, S. H. Yang, *J. Experi. Nanosci.* **2007**, *2*, 23–56.
[15] a) J. Q. Qi, H. Y. Tian, L. T. Li, H. L. W. Chan, *Nanoscale Res. Lett.* **2007**, *2*, 107–111; b) J. F. Xu, W. Ji, Z. X. Shen, S. H. Tang, X. R. Ye, D. Z. Jia, X. Q. Xin, *J. Solid State Chem.* **1999**, *147*, 516–519.
[16] a) Y. Zhou, S. Kamiya, H. Minamikawa, T. Shimizu, *Adv. Mater.* **2007**, *19*, 4194–4197; b) A. A. Umar, M. Oyama, *Cryst. Growth Des.* **2007**, *7*, 2404–2409; c) G. H. Du, G. Van Tendeloo, *Chem. Phys. Lett.* **2004**, *393*, 64–69; d) W. Z. Wang, O. K. Varghese, C. M. Ruan, M. Paulose, C. A. Grimes, *J. Mater. Res.* **2003**, *18*, 2756–2759; e) X. Y. Song, H. Y. Yu, S. X. Sun, *J. Colloid Inter. Sci.* **2005**, *289*, 588–591; f) T. Yu, F. C. Cheong, C. H. Sow, *Nanotechnology* **2004**, *15*, 1732–1736.
[17] a) M. H. Cao, Y. H. Wang, C. X. Guo, Y. J. Qi, C. W. Hu, E. B. Wang, *J. Nanosci. Nanotech.* **2004**, *4*, 824–828; b) T. Yu, X. Zhao, Z. X. Shen, Y. H. Wu, W. H. Su, *J. Cryst. Growth* **2004**, *268*, 590–595; c) M. H. Cao, C. W. Hu, Y. H. Wang, C. Xu, C. Zheng, G. Wang, *Chem. Commun.* **2003**, 1884–1885; d) C. K. Xu, Y. K. Liu, G. D. Xu, G. H. Wang, *Mater. Res. Bull.* **2002**, *37*, 2365–2372.
[18] a) W. X. Zhang, X. G. Wen, S. H. Yang, *Inorg. Chem.* **2003**, *42*, 5005–5014; b) R. Yang, L. Gao, *Solid State Commun.* **2005**, *134*, 729–733.
[19] a) D. Chen, G. Z. Shen, K. B. Tang, Y. T. Qian, *J. Cryst. Growth* **2003**, *254*, 225–228; b) M. Vaseem, A. Umar, S. H. Kim, Y. B. Hahn, *J. Phys. Chem. C* **2008**, *112*, 5729–5735; c) J. W. Zhu, H. P. Bi, Y. P. Wang, X. Wang, X. J. Yang, L. D. Lu, *Mater. Lett.* **2007**, *61*, 5236–5238.
[20] X. C. Jiang, T. Herricks, Y. N. Xia, *Nano Lett.* **2002**, *2*, 1333–1338.
[21] Y. Chang, H. C. Zeng, *Cryst. Growth Des.* **2004**, *4*, 397–402.
[22] H. M. Xiao, S. Y. Fu, L. P. Zhu, Y. Q. Li, G. Yang, *Eur. J. Inorg. Chem.* **2007**, 1966–1971.
[23] X. Q. Wang, G. C. Xi, S. L. Xiong, Y. K. Liu, B. J. Xi, W. C. Yu, Y. T. Qian, *Cryst. Growth Des.* **2007**, *7*, 930–934.
[24] H. L. Xu, W. Z. Wang, W. Zhu, L. Zhou, M. L. Ruan, *Cryst. Growth Des.* **2007**, *7*, 2720–2724.
[25] S. Q. Wang, J. Y. Zhang, C. H. Chen, *Scripta Mater.* **2007**, *57*, 337–340.
[26] A. M. Cao, J. D. Monnel, C. Matranaga, J. M. Wu, L. L. Cao, *J. Phys. Chem. C* **2007**, *111*, 18624–18628.
[27] B. Liu, H. C. Zeng, *J. Am. Chem. Soc.* **2004**, *126*, 8124–8125.
[28] Y. Y. Xu, D. R. Chen, M. L. Jiao, K. Y. Xue, *Mater. Res. Bull.* **2007**, *42*, 1723–1731.
[29] R. Xu, T. Xie, Y. G. Zhao, Y. D. Li, *Cryst. Growth Des.* **2007**, *7*, 1904–1911.
[30] Z. P. Zhang, X. Q. Shao, H. D. Yu, Y. B. Wang, M. Y. Han, *Chem. Mater.* **2005**, *17*, 332–336.

Received: September 11, 2008
Published Online: November 25, 2008

